Low-Temperature Heat Capacity, Glass-Transition Cooperativity, and Glass-Structure Vault Breakdown in a Series of Poly(*n*-alkyl methacrylate)s

M. Beiner,[†] S. Kahle,[†,⊥] S. Abens,[‡] E. Hempel,[†] S. Höring,[§] M. Meissner,[‡] and E. Donth*[,†]

Universität Halle, Fachbereich Physik, 06099 Halle (Saale), Germany; Hahn-Meitner-Institut, Glienicker Strasse 100, 14109 Berlin, Germany; and Universität Halle, Fachbereich Chemie, 06099 Halle (Saale), Germany

Received September 5, 2000; Revised Manuscript Received May 24, 2001

ABSTRACT: Heat capacity in the 1 K range and close to T_g was studied in a series of poly(*n*-alkyl methacrylate)s, PnAMA, including some random copolymers. We report on two findings: (i) The glass transition temperature T_g and the cooperativity of the α process that freezes-in at T_g, $N_\alpha(T_g)$, decrease smoothly between methyl (PMMA) and hexyl member (PnHMA); the cooperativity from $N_\alpha(T_g) = 35$ to $N_\alpha(T_g) \approx 1$. (ii) The tunnel density measured in the 1 K range as c_1 constant of the heat capacity function increases between PMMA and the ethyl member (PEMA), shows, after a maximum near PEMA, a sharp drop (factor of 6) to the butyl member (PnBMA), and remains constant at a low level up to the octyl member (PnOMA). The cooperativity of the α process near T_g and the tunnel density will be correlated assuming that freezing-in (vitrification) fixes the dynamic heterogeneity in the self-organized equilibrium liquid near T_g. We try to explain how freezing of dynamic heterogeneities in the PnAMA series is responsible for the trend in the tunnel density including the sharp drop: Freezing-in of cooperativity shells around Glarum defects forms some vaults that enlarge the free volume near these defects in comparison to a situation without vaults. The maximum in c_1 is promoted by this additional free volume; the drop in c_1 is caused by a vault breakdown effect if the cooperativity shell is too small for vault formation, $N_\alpha(T_g) < 15$.

Introduction

A characteristic feature of glasses such as amorphous polymers, biopolymers, small molecule liquids, or silicate glasses is in contrast to crystalline solids, a non-Debye behavior of the heat capacity near and below 1 K caused by low-energy excitations.[1−3] In the tunneling model[4,5] these excitations are described on a phenomenological basis by tunneling systems (TS). In the simplest case, such a tunneling system can be represented by a particle in a double-well potential. At low temperatures only the ground states in both wells are relevant. Because of the random structure elements of glasses, the characteristic parameters of the TS exhibit a wide distribution. This parameter distribution leads to a nearly linear contribution, c_1T, to the heat capacity in glasses at temperatures near and below 1 K,

$$c_p(T) \approx c_1T + c_3T^3 \tag{1}$$

where c_3T^3 is the Debye term of vibrations.

The tunnel density $\bar{P}$ in glasses usually decreases with increasing glass temperature T_g (cf. the full symbols in Figure 1a). The tunnel density is the number of TS per volume and per energy unit. Other measures are the number of TS per volume, n_0 of order 10^{17} cm^{-3}, corresponding to an average distance $d_0 = n_0^{-1/3}$ of about 10 nm between neighbor TS, or the tunnel fraction n_{TS} of order 10^{-5} per molecular unit. The $\bar{P} \approx n_0/k_BT_0$ values are on the order of $\bar{P} \approx 10^{23}\text{m}^{-3}/1.38 \times 10^{-23}$ J $\approx 7 \times 10^{45}$ J^{-1} m^{-3} for $T_0 = 1$ K. Assuming that the TS are effectively localized in the 1 K temperature range (double well distance $d \ll d_0$ and no effective coupling between neighbor TS near T_0), the specific heat contribution is additive:

$$c_1 \sim \bar{P} \sim n_0 \sim n_{TS} \tag{2}$$

The standard explanation for the $\bar{P}$ decrease with T_g is the large width assumed for the tunnel barrier energy distribution: For a uniform distribution between 0 and k_BT_g one gets $\bar{P} \sim 1/T_g$ for $n_0 =$ constant. This trend is reported for several substance classes in the literature, although the slope is usually steeper than d log $\bar{P}$/d log $T_g = -1$.

The idea of our study is to find a relationship between the tunnel density and the dynamic heterogeneity[6] as expressed by the cooperativity in the polymer melt that freezes-in at T_g. According to Adam and Gibbs,[7] glass formers above T_g are characterized by a self-organization in the liquid forming cooperatively rearranging regions, CRRs. The CRR size will be described by a volume $V_\alpha = \xi_\alpha^3$, with ξ_α being the characteristic length and N_α being a cooperativity, i.e., the number of particles (monomeric units for flexible polymers) inside an average CRR. Adam and Gibbs claimed that the optimization in the equilibrium liquid above T_g forms CRRs with increasing size for decreasing temperatures T ($> T_g$). The CRR volume V_α and cooperativity N_α can be determined from dynamic calorimetry using a fluctuation approach.[8]

[†] Universität Halle, Fachbereich Physik.
[‡] Hahn-Meitner-Institut.
[§] Universität Halle, Fachbereich Chemie.
[⊥] Present address: Institut für Festkörperforschung, Forschungszentrum Jülich GmbH, 52425 Jülich, Germany.
* Corresponding author. E-mail: donth@physik.uni-halle.de.

10.1021/ma001535f CCC: $20.00
Published on Web 07/11/2001

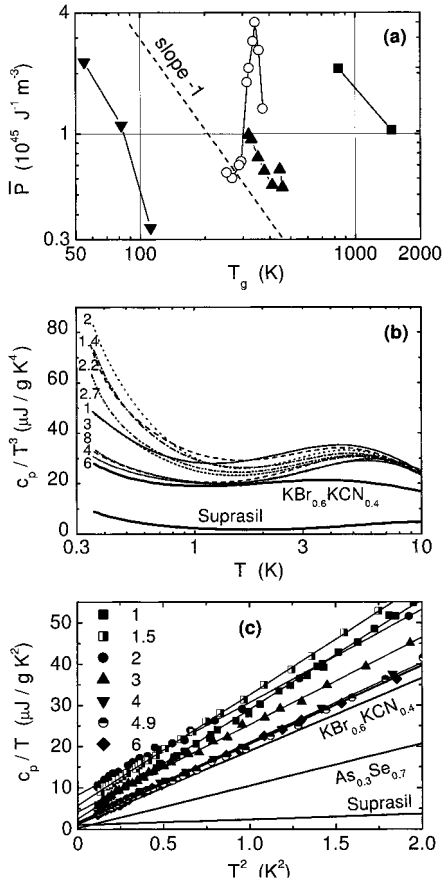

Figure 1. (a) Density of tunneling systems $\bar{P}$ in glasses as a function of glass temperature T_g. (▼) Orientational glass system $KBr_{1-x}KCN_x$ ($x = 0.2-0.6$,[35] T_g is sometimes substituted by the "dipolar freezing temperature"). (▲) Tetrahedrally bounded glass system As_xSe_{1-x} ($x = 0-0.5$).[47] (■) Silica glasses (BK7 and Suprasil).[22] The open circles O are the result of this paper for the poly(*n*-alkyl methacrylate)s (alkyl: methyl to octyl, including some random copolymers). (b) Specific heat capacity curves for the methacrylate polymer series and two other glasses in a c_p/T^3 vs log T diagram. The labels indicate the C numbers of the *n*-alkyl side groups (Table 1). The original data points (about 0.05 K spaced) are omitted for clarity. The lines are polynomial data fits. (c) Specific heat capacity data for 0.35 K < T < 1.4 K in a c_p/T vs T^2 diagram for eight selected (for clarity) methacrylate polymers and for three inorganic glasses (for comparison). The labels indicate the C number.

We calculate N_α from a thermodynamic von Laue treatment[9,10] of thermal fluctuations[8]

$$N_\alpha(T) = RT^2\Delta(1/c_V)/M_0(\delta T)^2 \approx RT^2\Delta(1/c_p)/M_0(\delta T)^2 \quad (3)$$

with $\Delta(1/c_V) = (1/c_V)^{glass} - (1/c_V)^{liquid}$ the step of reciprocal specific heat capacity at constant volume across the dynamic glass transition (α process), $(\delta T)^2$ the mean square of temperature fluctuation contribution of the α process related to an average CRR, and M_0 the molecular weight (g/mol) of the particle. The cooperativity usually obtained at T_g is of order $N_\alpha(T_g) \approx 100$ particles.[8,11,12]

The series of poly(*n*-alkyl methacrylate)s, with alkyl = methyl (PMMA), ethyl (PEMA), ..., octyl (PnOMA), is a substance series that is parametrized by the number of carbons C in the *n*-alkyl group of the side chain (C = 1 for PMMA, $C = 2$ for PEMA, ..., $C = 8$ for PnOMA). It is a feature of the PnAMA series that not only the glass temperature T_g but also the cooperativity $N_\alpha(T_g)$ decreases systematically with the increasing C number of carbons in the alkyl group of the side chain.[9,13,14]

The aim of this paper is to report on a combination of c_1 with $N_a(T_g)$, i.e., the low-temperature specific heat to determine the linear specific heat coefficients c_1 of eq 1, with the dynamic heat capacity near the glass temperature T_g to determine the glass transition cooperativity $N_\alpha(T_g)$ of eq 3, for the methacrylate polymer series between methyl and octyl members. Some random copolymers are included to get more data points in ranges of interest. An explanation of the relation between low-temperature properties and the cooperativity at T_g is attempted using a vault concept for vitrification of dynamic heterogeneity near T_g, introduced in ref 15 and described in detail in ref 16.

Experimental Section

1. Polymer Samples. The methyl, ethyl, propyl, and butyl samples of the PnAMA series were purchased from Polyscience Inc. The nonyl sample is a commercial product of the Polymer Source Inc. and was synthesized by living polymerization. The hexyl and octyl members were kindly provided by Dr. G. Meier (MPI-P Mainz/FZ Jülich) and Drs. T. Wagner and W. Steffen (MPI-P Mainz), respectively. Details about their synthesis are published elsewhere.[17,18] The pentyl and heptyl members as well as four random methyl−ethyl, ethyl−propyl, and butyl−hexyl copolymers were synthesized by free radical polymerization in toluene solution using α,α′-azoisobutyronitrile as an initiator.

Molecular weights, $\bar{M}_w$ and $\bar{M}_n$, tacticity, glass temperature T_g, and composition for the random copolymers are listed in Table 1. The molecular weights were determined by size exclusion chromatography. Tacticities were obtained from ^{13}C NMR measurements on the samples solved in nondeuterated THF. The pentyl, heptyl, and nonyl samples, additionally studied by DSC, also have a high molecular weight ($\bar{M}_n$ = 70−250 kg/mol). Similar tacticities (78 ± 5% syndiotactic diades) are expected for samples from free radical polymerization.

2. Low-Temperature Calorimetry. *Instrumentation and Measurements.* A new commercial relaxation type calorimeter[19] was used in the temperature range $T = 0.35-15$ K. The sample mass was $m \approx 10-30$ mg, and typical sample dimensions were $5 \times 5 \times 1.5$ mm^3. The samples were thermally contacted using ≈500 μg grease to the sapphire calorimeter chip. The preparation procedure and cooling rate were the same for all investigated polymers.

The c_p measurement is based on the evaluation of the temperature vs time response of the chip thermometer due to a step-function like constant heat flow P generated by a thin film heater on the sapphire chip which is weakly linked by a thermal resistance R_{th} to the thermal bath at T_0. The heat capacity is calculated from the exponential time constant τ of the temperature rise and the subsequent equilibrium temperature gradient $\Delta T = PR_{th}$ between the chip and the thermal bath. For the PnAMA samples (and other soft materials, as well) below 1 K, the thermal boundary resistance between the sample and the sapphire calorimeter increases proportional to T^{-3} and becomes comparable to the thermal resistance R_{th} of the tungsten wires forming the weak thermal link between the chip and the bath. Thus, the temperature vs time profiles are no more single exponential but can be described by two exponential contributions. According to an analysis and approximation formulas given by Shepherd,[20] all PnAMA heat capacity data below 5 K have been evaluated from a double-exponential fitting procedure to the measured temperature profiles.

Data Evaluation. A heat capacity contribution from the calorimeter (including a thin film W-heater and resistance

Table 1. Sample Characterization

sample[a]	T_g (K)	M_0 (g/mol)	$\bar{M}_w$ (kg/mol)	$\bar{M}_n$ (kg/mol)	tacticity (% syndio)	mol %	
1	379	100	86	33	79		Polyscience Inc.
1.4[b]	364	105	820	287	84	61/39	this work
2	343	114	154	81	78		Polyscience Inc.
2.2[b]	341	117	703	251	83	81/19	this work
2.7[b]	330	124	649	246	83	28/72	this work
3	324	128	283	61	75		Polyscience Inc.
4	298	142	160	76	78		Polyscience Inc.
4.9[b]	289	156	333	225	84	54/46	this work
6	253 ± 2	170	178	80	78		MPI-P Mainz
8	243 ± 5	184	154	70			MPI-P Mainz

[a] The sample symbol is the (average) C number of the *n*-alkyl group. [b] Random copolymer.

thermometer chip) was subtracted. This contribution is between ≈3% (at 1 K) and ≈ 7% (at 0.35 K) to the total heat capacity. PMMA c_p data at lower temperatures 60 mK < T < 600 mK from the literature[21] are about 20% higher in the overlap temperature range with our data. This difference is possibly caused by tacticity differences between the two PMMA samples.

The tunnel density $\bar{P}$ was calculated from the linear contribution to the low-temperature heat capacity

$$c_1 = (\pi^2 {k_B}^2 \bar{P}/6\rho)\{1.046 + \ln(2k_B T/\Delta_{0,\,\min}\} \qquad (4)$$

for $T > \Delta_{0,\,\min}/k_B$;[22] ρ is the mass density. As our c_p data are limited to $T \geq 0.35$ K, the deviation from the $c_p \sim T^1$ proportionality is small. We used, therefore, the approximation $\Delta_{0,\min} = 1$ mK and $T = T_0 = 0.5$ K in the correction term in the brackets of eq 4, {...} ≈ 8.

3. Dynamic Calorimetry near T_g. *Instrumentation and Measurements.* A DSC7 instrument from Perkin-Elmer was used in conventional (DSC) and in temperature-modulated (TMDSC) mode. The same samples were used for low-temperature and dynamic calorimetry. All samples were dried under vacuum for 12 h at a temperature of about $T = T_g + 80$ K. The sample weights were about 10 mg, and all samples were annealed prior to the measurements to yield a well-defined equilibrium state.

In the DSC mode a cooling−heating cycle between $T_g + 50$ K and $T_g - 100$ K with rates of $|dT/dt| = 10$ K/min was performed. The annealing time between cooling and heating runs was 5 min.

TMDSC experiments were carried out in saw-tooth-like modulation with a temperature amplitude $T_a = 0.2$ K. The modulation period was $t_p = 60$ s ($\omega = 2\pi/t_p = 0.105$ rad s^{-1}), and the underlying cooling rate was $\dot{T} = 0.5$ K/min. The magnitude of complex heat capacity $|c_p^*|$ and the phase angle δ were determined from the dynamic part of heat-flow rate according to ref 23.

The temperature scale of the calorimeter was calibrated in the common way with indium, mercury, and cyclopentane, depending on the temperature range. The scale was checked in the TMDSC mode with the smectic A to nematic transition of the M24 liquid crystal.[24] The purge gas was nitrogen, and the flow rate was 1 L/h.

Data Evaluation. The evaluation of calorimetric data was aimed at getting the parameters for the fluctuation formula (3). For DSC these parameters are the glass temperature T_g, the $\Delta(1/c_p)$ step value, and the width (dispersion) of the transformation interval δT in equilibrium. T_g was calculated from the $c_p(T)$ curve by an equal-area construction using two tangents, far below and far above the transformation interval.[25] Partial freezing-in is corrected by a modified Narayanaswamy Moynihan (MNM) procedure. The Kohlrausch parameters β_{KWW} obtained from the MNM procedure were used to calculate equilibrium δT values. The details of the data evaluation are described in refs 11 and 13.

The accuracy of the cooperativities obtained from DSC data was estimated to be (+100%, −50%)[11] and that for N_α values from TMDSC somewhat smaller (±50%). In the fluctuation formula for the cooperativity N_α, eq 3, c_V was replaced by c_p. [Individual c_V/c_p correction factors for poly(*n*-alkyl methacrylate)s were not available. An average correction term was suggested as $c_V/c_p \approx 0.74 \pm 0.22$.[11] To avoid additional uncertainties and confusion, this correction was not made.]

For TMDSC the dynamic glass temperature T_ω and the mean temperature fluctuation δT^2 for eq 3 were calculated from a Gaussian fit to the imaginary part of complex heat capacity at given frequency ω,

$$c_p''(T) = \text{const} \exp[(T - T_\omega)^2/2(\delta T)^2] \qquad (5)$$

The reason for using this formula is in detail explained in example 1 of section 3.3 in ref 16. The experimental uncertainties of the δT values (±10%) come mainly from uncertainties of the Gaussian fit. The uncertainty of $\Delta(1/c_p)$ (±15%) results mainly from uncertainties of the tangent construction (±10%). Further details are described in ref 11.

The correction from a polyethylene-type nanophase[26] to $\Delta(1/c_p)$ was also neglected, because no information about the volume fraction of these nanophases are at present available. This correction is estimated from the size of the alkyl groups to be smaller than 30% for $C \leq 6$, decreasing to zero for $C \lesssim 3$.

In summary, all the uncertainties of the N_a values, although large, are much smaller than the systematic decrease of N_a from PMMA to PnHMA (Table 2 and Figure 3b).

Results

Dynamic Calorimetry (DSC, TMDSC) near the Glass Temperature T_g. Two examples for dynamic calorimetry near T_g by DSC (differential scanning calorimetry) and TMDSC (temperature-modulated DSC) are shown in Figure 2, for $C = 2$ (PEMA) and $C = 5$ (PnPeMA). The data for the parameters used in eq 3 with the approximations of section 2 are listed in Table 2.

The cooperativities are calculated from DSC (at $T = T_g$) and TMDSC (at $T = T_\omega$) in the c_p approximation of eq 3, $\Delta(1/c_p) \approx \Delta(1/c_V)$. The differences (Figure 3a) between DSC and TMDSC cooperativities are significant and mainly due to the temperature difference between T_g and T_ω of about 5 K. We must describe how a reasonable series of cooperativity $N_\alpha(T_g)$ values (Figure 3b) at the freezing-in can be obtained from these data and how special disadvantages[27] of both methods, DSC and TMDSC, can be avoided. We use equilibrium cooperativities at T_g, $N_\alpha(T_g)$ (○ symbols in Figure 3a,b), determined from the TMDSC cooperativities at T_ω with a correction from the temperature difference between T_ω and T_g. The temperature dependence of cooperativity $N_\alpha(T)$ was approximated[28,29] by

$${N_\alpha}^{1/2}(x) = A(1 - x)/x \qquad (6)$$

with x a reduced temperature between Vogel tempera-

Table 2. Calorimetric Parameters from DSC and TMDSC

	DSC			TMDSC[a]			
sample	T_g (K)	$\Delta(1/c_p)$ (10^{-3} g K/J)	δT (K)	T_ω (K)	$\Delta(1/c_p)$ (10^{-3} g K/J)	δT (K)	corrected[e] $N_\alpha(T_g)$
1	379	85	3.6	383	86	6.2	36
1.4[d]	364	77	4.1	373	75	7.7	29
2	343	81	3.7	349	73	7.5	20
2.2[d]	341	70	4.4	347	68	7.5	18
2.7[d]	330	74	5.1	336	69	8.0	17
3	324	81	4.9	331	79	10.3	15
4	298	63	5.0	304	77	8.0	12
5	280	46	6.9	283	62	12.3	3
4.9[d]				289	50	9.9	2.3[c]
6	253 ± 2	85	5.8 ± 1.2	271	47	11.4	3
7				256 ± 2	84	19 ± 2	0.7[c]
8				247 ± 3	111	20.0 ± 3	0.7[c]
uncertainty	±1 K	±15%	±15%	±1 K	±15%	±10%	+100%[b] −50%[b]

[a] $\omega = 0.105$ rad s^{-1} from $t_p = 60$ s. [b] Absolute accuracy for $N_\alpha(T_g)$. [c] Uncorrected values from TMDSC. [d] Random copolymer. [e] Correction procedure see text and ref 27.

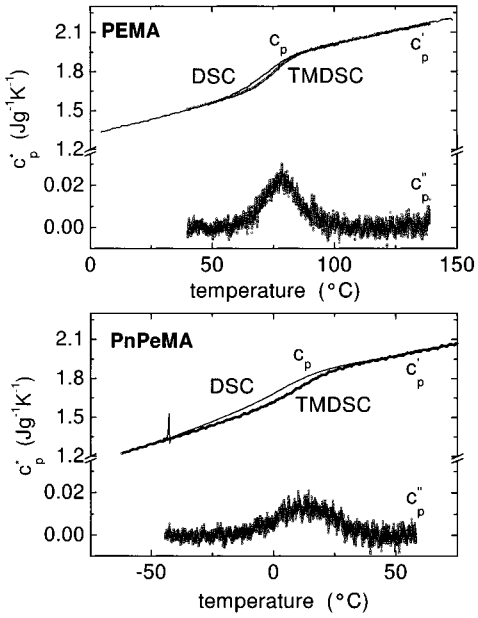

Figure 2. DSC and TMDSC thermograms for the ethyl member ($C = 2$) and the pentyl member ($C = 5$) of the PnAMA methacrylate polymer series. $c_p(T)$ from DSC for a cooling rate of $\dot{T} = -10$ K/min, $c_p^*(T) = c_p'(T) - ic_p''(T)$ TMDSC for a period $\tau_p = 60$ s (corresponding to $\omega = 0.105$ rad/s) with a slow underlying cooling rate of $\dot{T} = -0.5$ K/min.

ture T_0 ($x = 0$) and crossover temperature T_c ($x = 1$),

$$x(T) = (T - T_0)/(T_c - T_0) \qquad (7)$$

The $N_\alpha(T_\omega)$ values are used to determine the A constant in eq 6; $A = N_\alpha^{1/2}(x_\omega)x_\omega/(1 - x_\omega)$ with $x_\omega = x(T_\omega)$, and $N_\alpha^{1/2}(T_g)$ was determined by eq 6 as $N_\alpha^{1/2}(x_g)$ with $x_g = x(T_g)$. The T_0 and T_c values needed for correction are estimated from correlations of the scarce experimental information for our and related substances. Additional $N_a(T_g)$ uncertainties come from the uncertainties of crossover and Vogel temperatures, T_c and T_0, used in the x variable for the extrapolation by eq 6. The total accuracy is indicated by error bars in Figure 3b. The uncertainties from this procedure are large but still significantly smaller than the $N_\alpha^{1/2}$ change with the C number in our PnAMA series.

The $N_a(T_g)$ decrease of Figure 3b is interpreted by a systematic shift[30] of the crossover[31] temperature T_c in

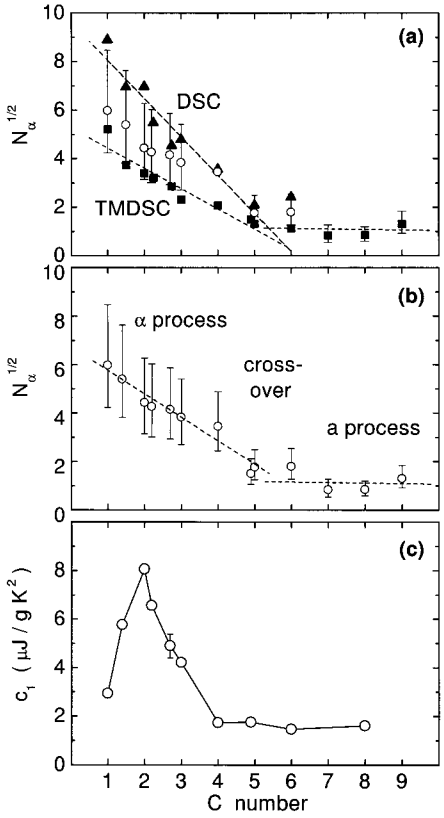

Figure 3. (a) Square root of cooperativity, $N_\alpha^{1/2}$, from eq 3 as a function of C number in the *n*-alkyl group of the methacrylate polymer series, PnAMA: ▲ from DSC for $|\dot{T}| = 10$ K/min; ■ from TMDSC for $\tau_P = 60$ s. O corrected values as described in the text and used in the final diagram of Figure 5b. Broken C numbers represent random copolymers (Table 1). (b) The corrected reference values of square root of glass transition cooperativity at T_g, $N_\alpha^{1/2}(T_g)$, for the PnAMA series. (c) Linear specific heat coefficients c_1 from low-temperature calorimetry.

direction to T_g. The crossover region divides the Arrhenius diagram into two parts: below T_c α and β processes are separated while above T_c only a single high-temperature a process is observed. For the lower members of the PnAMA series the shift is about one frequency decade per additional carbon in the alkyl part of the side chain. The glass temperature is reached ($T_c \approx T_g$) near $C = 6$, the hexyl member PnHMA.[32] The square root representation $N_\alpha^{1/2}(T_g)$ is chosen in Figure 2 according to our fluctuation approach[33] which indi-

Table 3. Boson Peak and c_1 and c_3 Constants in the PnAMA Series

C	T_{min} (K)	$(c_p/T^3)_{min}$ (μJ/(g K^4))	T_{max} (K)	$(c_p/T^3)_{max}$ (μJ/(g K^4))	R (eq 6)	c_1(μJ/(g K^2))	c_3 (μJ/(g K^4))
1	1.21	28.1	4.37	35.3	0.796	2.94	25.8
1.4[a]	1.61	29.2	4.42	31.4	0.856	5.77	26.6
2	1.61	26.0	4.66	33.2	0.783	8.07	23.0
2.2[a]	1.66	29.2	4.85	35.4	0.824	6.56	23.3
2.7[a]	1.56	26.6	5.02	33.7	0.789	4.90	22.0
3	1.52	24.9	5.24	32.9	0.757	4.22	21.1
4	1.21	21.6	5.43	32.9	0.655	1.73	19.3
4.9[a]	1.18	19.9	5.60	28.7	0.693	1.76	18.5
6	1.25	20.4	5.69	29.6	0.687	1.47	19.1
8	1.35	20.1	6.07	29.7	0.674	1.61	19.6

[a] Random copolymer.

cates $N_\alpha^{1/2} \sim (T_c - T)$ for $T < T_c$, consistent with experimental findings for other substances[34] (see eq 6).

Low-Temperature Heat Capacities. The low-temperature heat capacities of our PnAMA series are shown in a c_p/T^3 vs log T diagram (Figure 1b). In this plot the Debye vibration contribution c_3T^3 would be a horizontal line. All PnAMA samples have a more or less steep slope at lower temperature, indicating the linear term in specific heat, c_1T, and a significant boson peak between $T = 3$ K and $T = 10$ K (Table 3). The curves for the orientational glass $KBr_{0.6}KCN_{0.4}$[35] and Suprasil[22] in Figure 1b are given for comparison.

The c_1 constants are determined from the y-axis intercept in the c_p/T ($= c_1 + c_3T^2$) vs T^2 diagram (Figure 1c); the Debye term c_3 constants are determined from the slope in this diagram. Both the c_1 and c_3 constants are also listed in Table 3. Three inorganic glasses are included in Figure 1c for comparison.

The main result of our paper is displayed in Figure 3c: The c_1 constant as a function of the *n*-alkyl C number of the PnAMA series shows a clear maximum near $C = 2$ (PEMA), a sharp drop by a factor of 6 between $C = 2$ and $C = 4$ (PnBMA), and low constant values of order $c_1 = 1.5$ μJ/(g K^2) up to $C = 8$ (PnOMA). Note that the maximum and the drop are not at the $a-\alpha\beta$ process crossover ($C \approx 6$). The random copolymers fit into the general picture; i.e., the c_1 values are "insensitive" to random copolymerization. A similar maximum is indicated in previously reported[36] mechanical loss data for $C = 1$, 2, and 4.

The c_3 constant decreases with increasing side chain length for $C \lesssim 4$ and has a nearly constant value for $C > 4$ (Figure 4a). Note that the c_3 trends change at $C \approx 4$ or $N_\alpha \approx 12$, i.e., at a slightly smaller C number as the trend change in cooperativity ($C \approx 6$ (Figure 3b) where $T_c \rightarrow T_g$). The general trend for the Sokolov ratio R and fragility m (Figure 4b,c) is similar.

The Sokolov ratio R for the Boson peak[37] is defined as

$$R = (c_p/T^3)_{min}/(c_p/T^3)_{max} \leq 1 \qquad (8)$$

No boson peak would correspond to $R = 1$, R decreases with increasing boson peak. In the PnAMA series, R decreases first with increasing C number and remains constant for $C \gtrsim 4$. The R behavior resembles the general fragility behavior (Figure 4c) in the same way as suggested by Sokolov:[37] higher boson peak for lower fragility. The fragility index m[38] is often defined as $m = \mathrm{d}\log\tau_\alpha/\mathrm{d}(T_g/T)|_{T=T_g}$. We used a "dynamic fragility" related to the TMDSC frequency ω,

$$m_\omega = \mathrm{d}\log\tau_\alpha/\mathrm{d}(T_\omega/T)|_{T=T_\omega} \qquad (9)$$

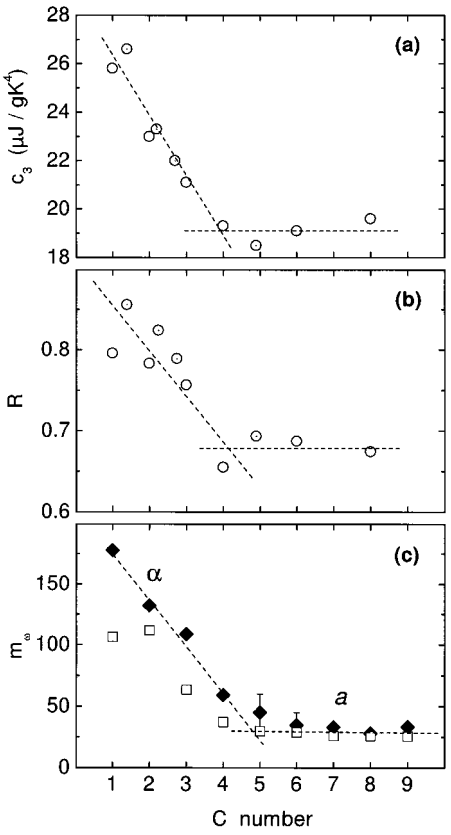

Figure 4. (a) c_3 constant, (b) Sokolov ratio R for boson peak, and (c) fragility m_ω as a function of the C number. The R and c_3 data are from low-temperature calorimetry for homopolymers (○) and random copolymers (⊙). The m_ω values are taken from dielectric data at T_ω ($\tau = 100$ s) (◆) and from shear data at T_ω ($\omega = 10$ rad/s) (□) using eq 9.

This fragility was determined for the PnAMA series from dielectric and shear[26] relaxation times in an Arrhenius plot. In general, $m_\omega < m(T_g)$, the reduction of m_ω to $m(T_g)$ would need traces of $\tau_\alpha(T)$ between T_ω and T_g, not yet available for several samples with the accuracy needed.

Supposing that the α_{PE} process in the PE nanophase[26] does not induce a large contribution to the boson peak, the main result from Figure 4b is that the occurrence of the boson peak is *not* restricted to large cooperativities near T_g and not restricted to the vitrification of the α process. Interpreting the relevant process for $C > 6$ (having a nearly constant fragility (Figure 4c) and cooperativity (Figure 3b)) as the high-temperature a process above the ($a-\alpha\beta$) process crossover temperature, we find that this a process is also connected with a large boson peak, at least after vitrification. The problem to

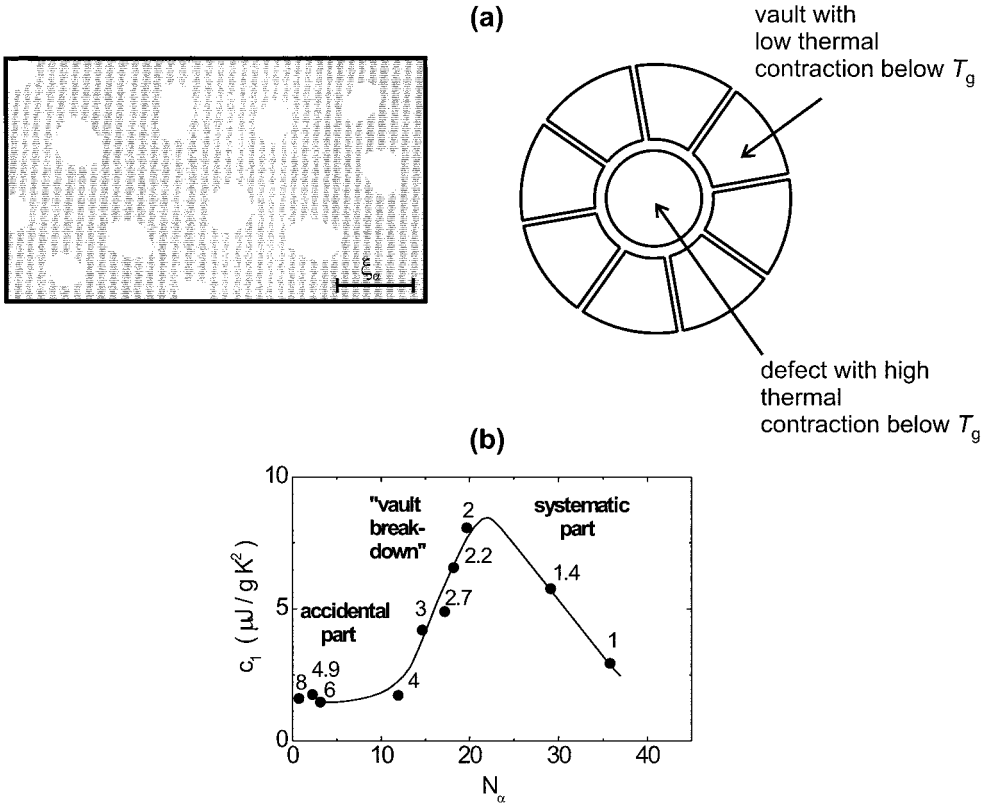

Figure 5. (a, left) Fluctuating pattern of dynamic heterogeneity[15] White: islands of mobility (Glarum Levy defects).[16] Gray: cell walls of low mobility (cooperativity shells). The size scale (characteristic length ξ_α) is given by the size of Adam Gibbs cooperatively rearranging regions (CRR) as determined by a von Laue treatment of thermal fluctuations, eq 3.[8] (a, right) Schematic picture of a molecular vault for glass structure. Details see text and ref 16. (b) Linear specific heat coefficients c_1 of eq 1 as a function of the glass transition cooperativity $N_\alpha^{1/2}(T_g)$ for the methacrylate polymer series, PnAMA. Broken *C* numbers represent random copolymers. For details see text.

determine the volume fractions of the nanophase separation is under way.[39]

The open symbols in Figure 1a indicate that the PnAMA series is an exception from the usual proportionality $c_1 \sim (1/T_g)$. The tunnel density shows a maximum near $C = 2$ (PEMA) and a sharp drop against the usual $(1/T_g)$ trend for the higher alkyl groups ($2 < C \leq 4$) while the T_g values decreases systematically. A comparison of parts b and c of Figure 3 indicates that the drop of the tunnel density between $C = 2$ and $C = 4$ may be connected with a glass transition cooperativity of about $N_\alpha(T_g) \approx 15$.

Discussion

In the framework of cooperativity concepts, glass-forming liquids are characterized by a temperature-dependent dynamic heterogeneity of the α process in the equilibrium liquid above T_g. We shall connect this heterogeneity with a fluctuating pattern of mobility (log $\omega(\mathbf{r},t)$) and of corresponding local free volume and local entropy.[15,16] It consists of islands of mobility in a cell structure of low mobility (Figure 5a). The islands of mobility are connected with Glarum defect diffusion.[40] The defect was treated by a Levy distribution,[15,16,33] reflecting the KWW function[27] used in the MNM model for the evaluation of the DSC data. The general occurrence of KWW functions at dynamic glass transition was first reviewed with respect to the Levy distribution of probability theory by Shlesinger;[41] see also ref 42. The cell walls of low mobility are now connected[15,16,43] with a cooperativity shell around each defect. The defect diffusion for the α process (below the crossover temperature) is assisted by the cooperativity shell. The size scale of the pattern is given by the size of Adam Gibbs cooperatively rearranging regions (CRR) as evaluated by eq 3.[8] This size was characterized by the characteristic length ξ_α or the cooperativity N_α.

We suggest a vault picture for explaining the maximum in the c_1 function of Figure 3c: A vault is the frozen cooperativity shell around a Glarum defect (Figure 5a). This defect is still working in a certain temperature interval below T_g and amplifies the small contrast of a concomitant density fluctuation pattern: The difference in thermal contraction between frozen shell and mobile defect generates additional free volume as long as the cooperativity is large enough to form a molecular vault around the defect. Below a minimal number $N_\alpha^{min}(T_g)$ of particles in the cooperativity shell no vaults can be formed ("vault breakdown effect"). Thus, no additional free volume can be generated inside vaults, and the systematic reason for the formation of tunneling systems disappears. We interpret the drop in the $c_1(N_\alpha)$ function, i.e. in the tunnel density, somewhere between $N_\alpha(T_g) = 20$ (PEMA) and $N_\alpha(T_g) = 12$ (PnBMA) as such a vault breakdown effect. This range is consistent with the hypothesis that a cooperativity larger than the first coordination shell is necessary for a vault. Using the N_α values as obtained from a Gibbs distribution analysis of the glass transition,[9] we would get N_α(Gibbs) values of order 500 for the drop of the c_1 function in Figure 3c. A relation to the first coordination shell would not longer be possible. The vault interpretation is therefore consistent with the von Laue approach leading to eq 3.

In the following we will give some details of our physical picture[16] as related to the results of this paper.

Dynamic Heterogeneity in the Liquid ($T > T_g$). A general phenomenon indicated by temperature-dependent cooperativity is called *disengagement of dynamic heterogeneity from molecular structure of the liquid*:[15,16] The cooperativity $N_\alpha(T)$ depends smoothly on temperature as indicated for example by eq 6. For glasses with high crossover frequency the cooperativity typically starts from $N_\alpha(T_g) \approx 100$ at T_g and decreases down to small values of order of one, $N_\alpha(T_c) \approx 1 \approx N_a$ at the crossover temperature T_c and above (for the *a* process at $T > T_c$). This behavior is also reflected in the N_α vs C plots of Figure 3a,b considering the special conditions in our PnAMA series. In this series the crossover frequency decreases from megahertz in PMMA ($C = 1$) to hertz in PnHMA ($C = 6$); i.e., the temperature difference $T_c - T_g$ decreases systematically with side chain length. Thus, the temperature dependence for a given substance is mapped here on the C number dependence at a given frequency. The first indication for disengagement is that there are, outside the uncertainties, no indications for a peculiarity in the $N_\alpha(T_g)$ function at a cooperativity of $N_\alpha \approx 10-15$, i.e., the number of particles in the first coordination shell of the liquid structure. The second indication is that smaller values than $N_\alpha = 10$ are reached when eqs 3 and 5 are also applied in the crossover region. A further indication for the disengagement is the fit of our random copolymers in the homopolymer PnAMA series (Figures 3, 4, and 5b).

The meaning of small cooperativities, $N_\alpha < 10$ or even $N_\alpha \approx 1 \approx N_a$ at and above T_c for crossover scenario I,[34] is a difficult problem that will be discussed in detail elsewhere.[9,16] The main idea is, starting from the $C_p = k_B \Delta S^2$ formula, that the experimental characteristic volume $V_\alpha = \xi_\alpha^3$ is related to the mobility pattern Figure 5a as obtained for entropy fluctuation of the α or *a* processes. In the crossover region and for the *a* process we use the picture of molecular cages as suggested by mode coupling theory (MCT). The diffusion is then that of one particle through a cage door. This is considered as a localized molecular event related to a cooperative rearrangement by relatively large amplitudes. The number of cage particles that "indirectly" (i.e., not so sensitive to entropy fluctuation) support the necessary cooperativity is not counted by N_α or N_a.

Vault Effect in the Glassy State ($T < T_g$).[15,16] Cooling the liquid below the glass temperature T_g, the actually existing dynamic heterogeneity in the self-organized liquid becomes finally a quasi-static pattern in the glassy state. It is the slow cooperativity shell, the cell walls of Figure 5a, which freezes first. There is a temperature interval below T_g where the mobility of the islands is still operating. The frozen cell walls then have a small thermal contraction and prevent the islands from "external" pressure or tension caused by freezing, like a vault. The mobile islands, however, still have a large thermal contraction in a certain temperature interval below T_g. The difference in thermal contraction "generates" additional free volume (in comparison to the situation with no vaults) that helps the islands to survive in this temperature interval below T_g and may systematically generate an additional part of such local low-density regions which are a condition for the tunneling systems (TS).

This "surviving temperature interval" (ΔT_S) can be estimated from the occurrence of short-time ($\lesssim$100 s) enthalpy recovery below T_g. The catchword is vault effect in enthalpy retardation. First calorimetric experiments[44] indicate that the fraction of enthalpy retardation for this vault effect is about 5% and that freezing effects in the islands are detectable down to $\Delta T_S \approx 30$ K below T_g for polystyrene and poly(vinyl acetate). First indications for such a short-time retardation in volume recovery can also be found in the diagrams of Kovacs' paper about structural relaxation.[45]

A molecular vault can only be formed by a minimal number of molecules (monomeric units here). This minimal number must be of the order of the first coordination shell of structure (Figure 5a). The vaults in glasses can hardly be detected by structure research because the density contrast of dynamic heterogeneity in the liquid is very small (of order $N_\alpha^{-1/\alpha}$ with $\alpha = \beta_{KWW}$ the Levy or Kohlrausch exponent;[15,16] example: $N_\alpha^{-1/\alpha} = 10^{-4}$ for $N_\alpha = 100$ and $\alpha = 1/2$). The different thermal contractions in the surviving temperature interval of glasses amplify the density contrast, but estimations indicate still a low contrast of at best 1% on the nanometer scale. The vault part of glass structure, important for e.g. the density of tunneling systems, mixed alkali effect in silicate and other glasses,[16] enthalpy recovery, and decrease of the effective ΔC_p step for an improvement of the Narayanaswamy Moynihan model,[46] is at present only indicated by indirect observations as here or, possibly, by computer experiments.

Vault Breakdown. The minimal cooperativity corresponding to the minimal number of particles that can form a vault in the glass state will be called *vault breakdown cooperativity*, $N_\alpha^{min}(T_g)$.

For larger cooperativities,

$$N_\alpha(T_g) > N_\alpha^{min}(T_g) \tag{10}$$

as mentioned above, the vault formation is a systematic reason for the formation of additional tunneling systems, TS. As we have one defect per CRR (one preponderating Levy component in the set of additive random variables for the partial systems of a single CRR[15]), the tunnel fraction $n_{TS} \propto 1/N_\alpha(T_g)$. Assuming a constant tunnel barrier distribution between 0 and $k_B T_g$, we get a *systematic part of the density of tunneling systems*

$$n_{TS} \approx T_0/T_g N_\alpha(T_g) \approx 10^{-5} \quad \text{for } N_\alpha(T_g) > N_\alpha^{min}(T_g) \tag{11}$$

with $T_0 \approx 1$ K.

For smaller cooperativities,

$$N_\alpha(T_g) < N_\alpha^{min}(T_g) \tag{12}$$

the systematic reason for additional tunneling system formation is absent, and we expect only a small *accidental part of tunneling density*. This part should also be observed in amorphous solids prepared without a glass transition.

If we apply this idea to our experimental results for the c_1 constant as a function of cooperativity (Figure 5b), the obtained vault breakdown cooperativity is $N_\alpha^{min}(T_g) \approx 10-20$, consistent with the number of particles that form the first coordination sphere of glass structure. The $N_\alpha(T_g)$ drop from a situation with vaults to a situation with no vaults is gradual which may be explained by

the amorphicity of structure and by a distribution[15] of CRR sizes, wide for small N_α.

In summary, the presented results for the PnAMA series can consistently be interpreted within the picture of dynamic heterogeneities which are formed in the self-organized equilibrium liquid above T_g, which are amplified by different expansion coefficients of vault and defect in a certain temperature interval below T_g, which are frozen-in to a quasi-static pattern some 10 K below T_g and which form, far below T_g, a systematic reason for tunneling systems in glasses near 1 K.

Conclusions

(i) The linear specific heat coefficient c_1 determined in the 0.35−1.4 K temperature range as a function of C number in the *n*-alkyl side group of a poly(*n*-alkyl methacrylate) series has a pronounced maximum near the ethyl member ($C = 2$).

(ii) The sharp drop of c_1 for C numbers between 2 and 4 (ethyl and butyl member) is interpreted as "vault breakdown" of the glass structure because the cooperatively rearranging regions CRR in the liquid at glass temperature T_g become too small for vault formation by the first coordination shell.

(iii) We suggest a distinction between two parts of the tunnel density: an accidental part due to the general amorphicity (here of order $\bar{P} \approx 0.5 \times 10^{45}$ J^{-1} m^{-3}) and a systematic part due to contributions resulting from the vault formation in the glass below T_g (here up to $\bar{P} \approx 4 \times 10^{45}$ J^{-1}m^{-3}).

(iv) Experimental results for the cooperativity at T_g in the PnAMA series can be understood as indication for a disengagement of dynamic heterogeneity from liquid structure.

(v) The existence of the boson peak in the 3−10 K temperature range also for small cooperativities down to a few particles and, even for the *a* process above the $a-\alpha\beta$ crossover, indicates that its occurrence is not caused by the cooperativity of the α process and its typical characteristic length of order 2−3 nm.

Acknowledgment. We thank Professor R. O. Pohl, Cornell University, Professor S. Hunklinger, Universität Heidelberg, and Dr. P. Strehlow, PTB Berlin, for discussions about a previous draft of the paper and about conceptual points. We are grateful to C. Schicktanz and Professor K. Schlothauer, FH Merseburg, for tacticity measurements. Financial support by the Deutsche Forschungsgemeinschaft DFG is acknowledged. E.D. also thanks the Fonds Chemische Industrie FCI.

References and Notes

(1) Zeller, R. C.; Pohl, R. O. *Phys. Rev. B* **1971**, *4*, 2029. Hunklinger, S.; Raychaudhuri, A. K. *Prog. Low Temp. Phys.* **1986**, *9*, 267. Phillips, W. A. *Rep. Prog. Phys.* **1987**, *50*, 1657. Berret, J. F.; Meissner, M. *Z. Phys. B* **1988**, *70*, 65.
(2) *Amorphous Solids*; Topics in Current Physics Vol. 24; Phillips, W. A., Ed.; Springer: Berlin, 1984.
(3) Esquinazi, P., Ed. *Tunneling Systems in Amorphous and Crystalline Solids*; Springer: Berlin, 1998.
(4) Anderson, P. W.; Halperin, B. I.; Varma, C. M. *Philos. Mag.* **1972**, *25*, 1.
(5) Phillips, W. A. *J. Low Temp. Phys.* **1972**, *7*, 351.
(6) Ediger, M. D. *Annu. Rev. Phys. Chem.* **2000**, *51*, 99.
(7) Adam, G.; Gibbs, J. H. *J. Chem. Phys.* **1965**, *43*, 139.
(8) Donth, E. *J. Non-Cryst. Solids* **1982**, *53*, 325.
(9) Donth, E.; Hempel, E.; Schick, C. *J. Phys.: Condens. Matter* **2000**, *12*, L281.
(10) Donth, E. *J. Phys.: Condens. Matter* **2000**, *12*, 10371.
(11) Hempel, E.; Hempel, G.; Hensel, A.; Schick, C.; Donth, E. *J. Phys. Chem. B* **2000**, *104*, 2460.
(12) Donth, E.; Huth, H.; Beiner, M. *J. Phys.: Condens. Matter* **2001**, *13*, L451.
(13) Hempel, E.; Kahle, S.; Unger, R.; Donth, E. *Thermochim. Acta* **1999**, *329*, 97.
(14) Hempel, E.; Beiner, M.; Renner, T.; Donth, E. *Acta Polym.* **1996**, *47*, 525. Zeeb, S.; Höring, S.; Garwe, F.; Beiner, M.; Hempel, E.; Schönhals, A.; Schröter, K.; Donth, E. *Polymer* **1997**, *38*, 4011. Garwe, F.; Schönhals, A.; Lockwenz, H.; Beiner, M.; Schröter, K.; Donth, E. *Macromolecules* **1996**, *29*, 247.
(15) Donth, E. *Acta Polym.* **1999**, *50*, 240.
(16) Donth, E. *The Glass Transition. Relaxation Dynamics in Liquids and Disordered Materials;* Springer: Berlin, 2001.
(17) Giebel, L.; Meier, G.; Fytas, G.; Fischer, E. W. *J. Polym. Sci., Part B: Polym. Phys.* **1992**, *30*, 1291. Meier, G.; Kremer, F.; Fytas, G.; Rizos, A. *J. Polym. Sci., Part B: Polym. Phys.* **1996**, *34*, 1391.
(18) Beiner, M.; Korus, J.; Donth, E. *Macromolecules* **1997**, *30*, 8420.
(19) MagLab^{HC} calorimeter, manufactured by Oxford Instruments SRD, Tubney Woods, Abingdon, UK.
(20) Shepherd, J. P. *Rev. Sci. Instrum.* **1985**, *56*, 273.
(21) Stephens, R. B. *Phys. Rev. B* **1976**, *13*, 852. Nittke, A.; et al. *J. Low Temp. Phys.* **1995**, *98*, 517.
(22) Meissner, M.; Strehlow, P. In *Proceedings of the 21st International Conference on Low-Temperature Physics*, Prague, CZYPAO **1996**, *46 (S4)*, 2233. Abens, S.; Meissner, M.; Strehlow, P., to be published.
(23) Weyer, S.; Hensel, A.; Schick, C. *Thermochim. Acta* **1997**, *304/305*, 267.
(24) Hensel, A.; Schick, C. *Thermochim. Acta* **1997**, *304/305*, 229.
(25) Moynihan, C. T.; Easteal, A. J.; DeBolt, M. A.; Tucker, J. *J. Am. Ceram. Soc.* **1976**, *59*, 12.
(26) Beiner, M.; Schröter, K.; Hempel, E.; Reissig, S.; Donth, E. *Macromolecules* **1999**, *32*, 6278.
(27) The DSC cooperativities have the advantage that they are obtained directly at the glass temperature T_g where the samples freeze. The disadvantage is their determination from a cooling curve using a modified (WLF scaling instead of Arrhenius scaling) Narayanaswamy Moynihan program (MNM).[13] This program is stabilized over a wide time scale by Moynihan's suggestion to use a Kohlrausch−Williams−Watt (KWW) function for the enthalpy retardation, $\exp(-(t/\tau(T))^{\beta_{KWW}})$, $0 < \beta_{KWW} \leq 1$, with the stretching exponent β_{KWW} = constant. This implies, for DSC trace evaluation, that a broad informative temperature interval $\tilde{\Delta}\tilde{T}$ of about $\tilde{\Delta}\tilde{T} \approx$ 20 K is included in the evaluation. This is only reasonable if the retardation is thermorheologically simple in this $\tilde{\Delta}\tilde{T}$ interval, i.e., that the retardation can be described with a nearly constant β_{KWW} value. This is not fulfilled for some of our samples,[43] since peculiarities[32] at the crossover region enter the informative temperature interval. The TMDSC cooperativities have the advantage that they are obtained from an isochronous section of the equilibrium dispersion zone (cooperative α process for $C < 5$, high-temperature *a* process for $C > 7$). The informative temperature interval is much smaller than from DSC, and therefore, the requirements to thermorheological simplicity are weak. The disadvantage is that the dynamic glass temperature T_ω for $\omega = 2\pi/60s$ is higher than the conventional glass temperature T_g, of course, and does not correspond to the actual freezing as first stage of forming the glass structure. The temperature difference $\Delta T_{\omega g} = T_\omega - T_g$ is of order $\Delta T_{\omega g} = 5$ K (Table 2).
(28) Korus, J.; Hempel, E.; Beiner, M.; Kahle, S.; Donth, E. *Acta Polym.* **1997**, *48*, 369.
(29) Huth, H.; Beiner, M.; Donth, E. *Phys. Rev. B* **2000**, *61*, 15092.
(30) Heijboer, J. *Stat. Dyn. Prop. Polym. Solid State* **1982**, *94*, 197.
(31) Williams, G. *Trans. Faraday Soc.* **1966**, *62*, 2091. Johari, G. P.; Goldstein, M. *J. Chem. Phys.* **1970**, *53*, 2372; **1970**, *54*, 2034; **1971**, *55*, 4245.
(32) Beiner, M.; Kahle, S.; Hempel, E.; Schröter, K.; Donth, E. *Europhys. Lett.* **1998**, *44*, 321.
(33) Donth, E. *J. Phys. I* **1996**, *6*, 1189. Donth, E.; Kahle, S.; Korus, J.; Beiner, M. *J. Phys. I* **1997**, *7*, 581.
(34) Kahle, S.; Korus, J.; Hempel, E.; Unger, R.; Höring, S.; Schröter, K.; Donth, E. *Macromolecules* **1997**, *30*, 7214.
(35) de Yoreo, J. J.; Knaak, W.; Meissner, M.; Pohl, R. O. *Phys. Rev. B* **1986**, *34*, 8828. Berret, J. F.; Meissner, M. In *Phonon Scattering in Condensed Matter*; Anderson, A. C., Wolfe, J. P., Eds.; Springer: Berlin, 1986; p 83.

(36) Hickel, W.; Kasper, G. *Cryogenics* **1988**, *28*, 230.
(37) Sokolov, A. P.; Rössler, E.; Kisliuk, A.; Quitmann, D. *Phys. Rev. Lett.* **1993**, *71*, 2062.
(38) Böhmer, R.; Ngai, K. L.; Angell, C. A.; Plazek, D. J. *J. Chem. Phys.* **1993**, *99*, 4201.
(39) Kabisch, O.; Reichl, S.; et al., to be published.
(40) Glarum, S. H. *J. Chem. Phys.* **1960**, *33*, 639.
(41) Shlesinger, M. F. *Annu. Rev. Phys. Chem.* **1988**, *39*, 269.
(42) Bendler, J. T.; Shlesinger, M. F. *J. Phys. Chem.* **1992**, *96*, 3970.
(43) Kahle, S.; Hempel, E.; Beiner, M.; Unger, R.; Schröter, K.; Donth, E. *J. Mol. Struct.* **1999**, *479*, 149.
(44) Weyer, S.; Schick, C. (Rostock), private communication, 2000. Hempel, E.; et al., unpublished results.
(45) Kovacs, A. J. *Fortschr. Hochpolym.-Forsch.* **1963**, *3*, 394.
(46) Gomez Ribelles, J. L.; Monleon Pradas, M. *Macromolecules* **1995**, *28*, 5867.
(47) Liu, X.; von Löhneysen, H. *Phys. Rev. B* **1993**, *48*, 486.

MA001535F